Spectroscopic study of debris mitigation with minimum-mass Sn laser plasma for extreme ultraviolet lithography

S. Namba[a)]
Graduate School of Engineering, Hiroshima University, 1-4-1 Kagamiyama, Higashi-Hiroshima, Hiroshima 739-8527, Japan

S. Fujioka, H. Nishimura, Y. Yasuda, K. Nagai, N. Miyanaga, Y. Izawa, and K. Mima
Institute of Laser Engineering, Osaka University, 2-6 Yamada-oka, Suita, Osaka 565-0871, Japan

K. Takiyama
Graduate School of Engineering, Hiroshima University, 1-4-1 Kagamiyama, Higashi-Hiroshima, Hiroshima 739-8527, Japan

An experimental study was made of a target consisting of the minimum mass of pure tin (Sn) necessary for the highest conversion to extreme ultraviolet (EUV) light while minimizing the generation of plasma debris. The minimum-mass target comprised a thin Sn layer coated on a plastic shell and was irradiated with a Nd:YAG laser pulse. The expansion behavior of neutral atoms and singly charged ions emanating from the Sn plasma were investigated by spatially resolved visible spectroscopy. A remarkable reduction of debris emission in the backward direction with respect to the incident laser beam was demonstrated with a decrease in the thickness of the Sn layer. The optimal thickness of the Sn layer for a laser pulse of 9 ns at 7×10^{10} W/cm^2 was found to be 40 nm, at which low-debris emission in the backward direction and a high conversion to 13.5 nm EUV radiation were simultaneously attained. © *2006 American Institute of Physics*.
[DOI: 10.1063/1.2199494]

Hot dense plasmas created by intense laser pulses have been extensively studied for use in various applications, such as next generation extreme ultraviolet lithography (EUVL),[1] x-ray microscopy,[2] and absorption spectroscopy.[3] Recently, much effort has been devoted to improving the EUV conversion efficiency (CE) in EUVL at 13.5 nm in a 2% bandwidth (BW). Water,[4] lithium,[5] xenon,[6,7] and Sn (Refs. 8 and 9) plasmas generated with high-power lasers are candidates for EUV light sources. An important consideration in realizing an EUVL system is solving the problems of contamination by debris and sputtering by ions on the first mirror of an EUV system. Various techniques to inhibit debris ablated from the target, such as a gas jet/buffer,[10,11] an electric shield,[12] and mass-limited targets,[4,12] have been proposed.

"Minimum-mass target" is an effective alternative method for eliminating the neutral atoms and low-ionized ions originating from the low-intensity wing of the laser spot as well as the deep layer from the target surface, with which almost all the atoms subjected to laser pulses could be turned into highly charged ions without additional emission of neutral atoms from the target.[13,14] The concept of the minimum-mass target is clearly different from that of the mass-limited target,[12] where EUV source material is solved in a liquid such as water that can be an alternative source of debris. In order to simultaneously attain low-debris emission and high CE to EUV radiation, the number of atoms in the target must be optimized. In addition, since volume recombination, responsible for regeneration of neutral atoms, may offset the advantages of a minimum-mass target, a strong understanding of the debris dynamics is essential for further progress in developing a debris-free EUV source.

Experiments were performed with a Nd:YAG laser pulse (wavelength 1064 nm, pulse width 9 or 2.5 ns) and minimum-mass targets consisting of Sn layers of 10–1300 nm thicknesses deposited on a plastic hollow sphere (thickness ~ 7 μm, diameter ~ 500 μm). The laser beam was focused by a lens, irradiating the target with a spot size of ~ 500 μm. Spectroscopic investigations were carried out using two time- and space-resolved optical systems. For one-dimensional (1D) measurement along the direction parallel to the incident laser, visible emissions were collected with a lens onto an optical bundle fiber. Spatially resolved spectra were measured with a spectrometer coupled with a temporally gated intensified charge coupled device (ICCD) camera. The other optical system, used for two-dimensional (2D) measurements, consisted of an interference filter [atom 452 nm ($5p^2$ ^1S-$6s$ ^1P) or Sn$^+$ ion 579 nm ($5d$ ^2D-$4f$ ^2F)] and the ICCD camera. It should be noted that the spectral intensity is in proportion to the population density of the excited level. EUV light was measured using an absolutely calibrated calorimeter (E-mon of Jenoptik) and a grazing incidence spectrometer. The spectral sensitivity of the EUV calorimeter, the spectral shape, and the measured angular distribution of the EUV emission were taken into account for the CE evaluation at 13.5 nm within a 2% BW emitted into 2π sr.[13] Ion stages and the energies of particles ejected from the plasma were measured with a Thomson parabola ion spectrometer.[14]

Figure 1 shows 1D spatially resolved spectra for Sn layers of 350 and 30 nm thickness. The horizontal and vertical axes correspond, respectively, to the wavelength (554–596 nm) and the spatial position. Laser pulses of 9 ns at 7×10^{10} W/cm^2 were used to irradiate the target in a direction from the top of the figures. The gate delay from the onset of the laser pulse and the gate width were set to 100
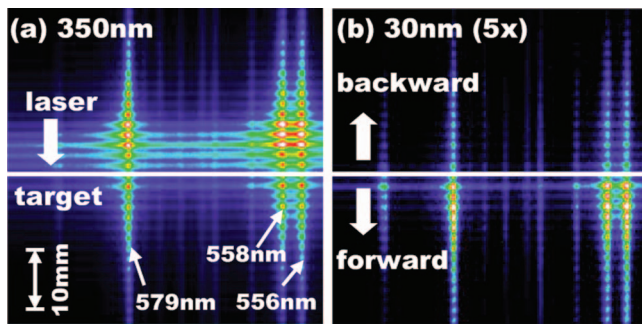
[a)]Electronic mail: namba@hiroshima-u.ac.jp

FIG. 1. (Color) 1D distribution of Sn⁺ ion-spectra for Sn (a) 350 nm and (b) 30 nm thick targets. The latter image is intensified by a factor of 5 for comparison. In this wavelength region, there are four bright Sn⁺ ion peaks at 556.2, 558.9, 579.7, and 579.9 nm, although the last two transitions blend together.

and 550 ns, respectively. The most remarkable aspect of the spectra is the influence of the Sn coat thickness. For the 350 nm thick target, the Sn⁺ ion spectrum showed maximum intensities at ~7 mm away from the target surface toward the backward direction [Fig. 1(a)], where the backward direction is defined as the opposite direction to the laser incidence. On the other hand, for the 30 nm layer, the Sn⁺ ions favorably expanded in the forward direction, as shown in Fig. 1(b). Similar spatial distributions were obtained for the atomic spectra.

Figures 2(a) and 2(b) show the dependence of the spectral intensities of 452 nm light, attributed to atoms, and 579 nm, attributed to Sn⁺ ions, on the thickness of the Sn layer. The output counts from the CCD obtained for the forward and backward directions were separately accumulated. For deposition layers thinner than 50 nm, the expansion of atoms and ions into the backward direction was dramatically restrained. The intensity at 452 nm for a 10 nm thick layer in the backward direction was 25 times weaker than that for a 1000 nm layer, while the 579 nm light intensity decreased by an even greater amount (by a factor of 140). It is also interesting that the ion spectral intensity decreases at a thickness of 40 nm. Here, it should be noted that the spectral intensities observed do not reflect the ground state densities of atoms and Sn⁺ ions. Nevertheless, considering that (1) for thinner targets almost all of the atoms are highly ionized as described below, (2) three-body recombination responsible for the populations of highly excited levels could dominate well after the laser irradiation, and (3) the excited states eventually decay to the ground state via collisional-radiative processes, the emission distribution is considered to be closely correlated with the spatial distribution of the resultant ground state. Hence, the results shown in Fig. 2 demonstrate that a spherical target with a thin Sn layer has the high potential to prevent neutral atoms and Sn⁺ ions from depositing on the first EUV mirror, which is located in the backward direction.

The dependence of the CE on the Sn thickness is shown in Fig. 2(c), indicating that the CE is almost constant (~1.2%) for the targets with a Sn coat of 30 nm or thicker. This result implies that layers more than 30 nm thick do not significantly contribute to the EUV output due to strong self-absorption.[13,14] Making a comprehensive assessment of the results obtained, the target with a Sn 40 nm layer is optimal for the present condition, at which the low-debris emis-
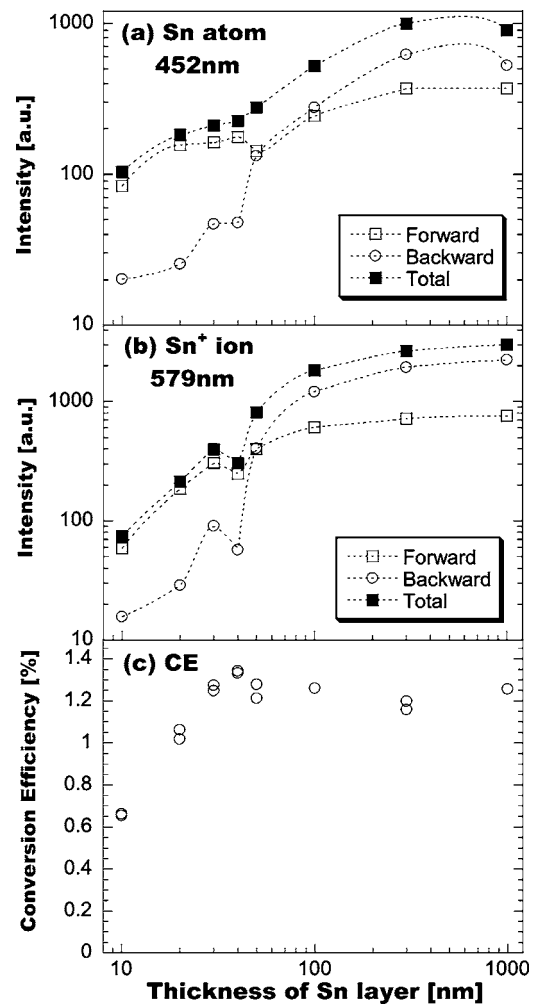

FIG. 2. Dependence of the intensities in the forward and backward directions on the Sn layer thickness for (a) neutral atoms (452 nm) and (b) Sn⁺ ions (579 nm). The CE at 13.5 nm as a function of thickness is shown in (c).

sion in the backward direction and the high CE to 13.5 nm radiation were simultaneously attained.

The forward expansions of atoms and Sn⁺ ions with thinner layer targets cannot be simply attributed to the laser-driven acceleration of the light target itself toward the forward direction.[15] In order to investigate the particle dynamics responsible for the forward expansion of the debris, 2D distributions of emission spectra were observed, and the results for targets with 30 and 50 nm layers are shown in Fig. 3(a). As is clearly seen, the forward emissions of atoms and Sn⁺ ions dominate backward emission. In contrast to the distributions of a neutral atom and Sn⁺ ion debris for thin Sn targets, EUV radiation is dominantly emitted toward the forward direction. The angular distribution which is not dependent upon the Sn thickness is fitted with $f(\theta) = 0.57 + 0.43 \cos^{1.31} \theta$, where θ is an angle with respect to the incident laser.

Ion energy spectra obtained with a Thomson parabola indicate that the energy distribution of highly charged ions shifts toward the high-energy side with a decrease in the Sn thickness. Even at a direction of 90° from the target normal, energetic ions in excess of 1 keV were observed using a charge collector.[14] Considering that the particles emitted from the target undergo collisional heating during expansion, this result suggests that for targets with thinner layers almost all of the atoms emitted toward the backward direction
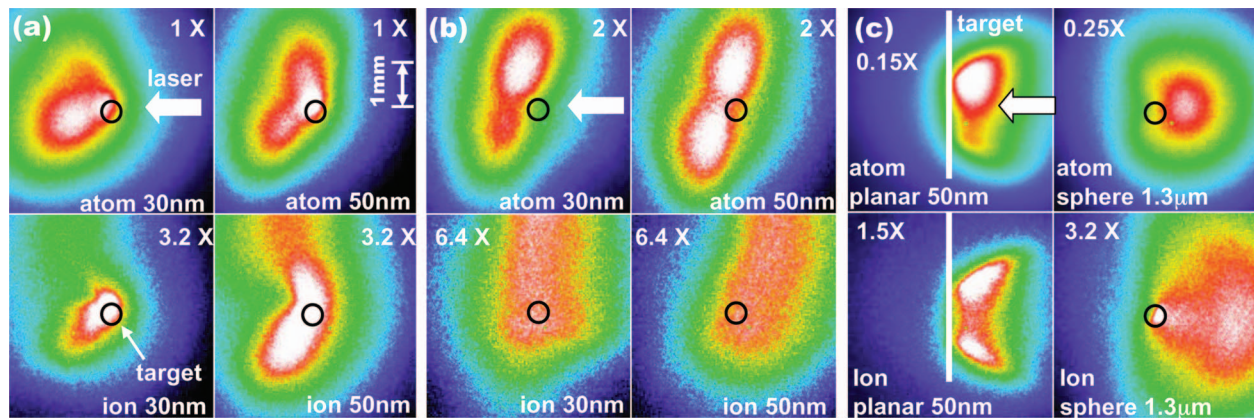
FIG. 3. (Color) 2D distributions of atomic and ionic spectra for (a) a hollow target irradiated with a 9 ns pulse, (b) a hollow sphere irradiated with a 2.5 ns pulse, and (c) a thin planar (50 nm) and a sphere target coated with 1300 nm thick Sn irradiated with a 2.5 ns pulse. The number shown in the inset of each frame represents an intensity multiplication factor.

should be highly ionized and thus few atomic and Sn$^+$ ionic emissions will be observed in this direction. Meanwhile, since the heat capacity is low for thinner targets, the atoms on the rear side (opposite the laser) can also be ablated due to the heating of the target surface by the laser pulse, followed by the interaction of the ejected atoms with the low-intensity wings of the laser profile as well as the hot plasma in the lateral direction. Consequently, a low-temperature plasma responsible for plasma emission, as described later, can be generated on the rear side of the target. With an increase in the Sn thickness, however, the heat capacity increases, resulting in less ablation at the rear side. In addition, since the deep layers of a thick target also contribute to generating the cold plasma, the backward emission dominates over the forward emission for thicker Sn layers.

The dependence of the 2D intensity distribution on the pulse width (2.5 ns, 7×10^{10} W/cm^2) was also investigated. The results for 30 and 50 nm layers are shown in Fig 3(b). The figure indicates that the particles are preferably emitted in the lateral direction. The spatially integrated intensity of the atomic spectrum for the 40 nm thick target was 3.6 times weaker than that for the 9 ns pulse. Moreover, for the 50 nm layer, bright ion emission was observed in the backward direction. The integrated intensity ratio of Sn$^+$ ions for the 9 ns pulse to that for the 2.5 ns pulse was around 2.5 for the 40 nm target. Nevertheless, the CE for the shorter pulse was greater by up to 1.8%.[13] Since the hydrodynamic behavior of Sn ions can be controlled using an external electromagnetic field, a short-pulse laser together with a minimum-mass target potentially allows the reduction of neutral atoms and solves the problem of debris contamination on EUV optics.

Finally, in Fig. 3(c) we show 2D profiles obtained for a thin Sn planar target (50 nm) with a laser pulse of 2.5 ns. Intense emission from the outside of the laser spot was observed, where a low-temperature plasma may have been produced due to the low-intensity wings of the laser spot. However, the optical emissions on the laser beam axis were weak, since the atoms could be highly ionized. Therefore, the atomic and ionic emissions observed can be considered to reflect the presence of cold plasma. Meanwhile, their genera-

tions at the plasma edge can be substantially suppressed by using a spherical target of the same diameter as the laser spot. The 2D distribution of a spherical target with a 1300 nm layer is also shown in Fig. 3(c). This demonstrates that the shape of a target plays an important role in debris emission.

[1] R. Service, Science **293**, 785 (2001).
[2] L. Malmqvist, L. Rymell, M. Berglund, and H. M. Hertz, Rev. Sci. Instrum. **67**, 4150 (1996).
[3] J. S. Hirsch, E. T. Kennedy, A. Neogi, and J. T. Costello, Rev. Sci. Instrum. **74**, 2992 (2003).
[4] C. Keyser, G. Schriever, M. Richardson, and E. Turcu, Appl. Phys. A **77**, 217 (2003).
[5] A. A. Andreev, T. Ueda, and J. Limpouch, Proc. SPIE **4343**, 789 (2001).
[6] H. Shield, S. W. Fornaca, M. B. Petach, M. Michaelian, R. D. McGregor, R. H. Moyer, and R. J. St. Pierre, Proc. SPIE **4688**, 94 (2002).
[7] A. Shimoura, S. Amano, S. Miyamoto, and T. Mochizuki, Appl. Phys. Lett. **72**, 164 (1998).
[8] H. Tanaka, A. Matsumoto, K. Akinaga, A. Takahashi, and T. Okada, Appl. Phys. Lett. **87**, 041503 (2005).
[9] P. A. C. Jansson, B. A. M. Hansson, O. Hemberg, M. Otendal, A. Holmberg, J. de Groot, and H. M. Hertz, Appl. Phys. Lett. **84**, 2256 (2004).
[10] L. Rymell and H. M. Hertz, Rev. Sci. Instrum. **66**, 4916 (1995).
[11] S. Bollanti, F. Bonfigli, E. Burattini, P. D. Lazzaro, F. Flora, A. Grilli, T. Letardi, N. Lisi, A. Marinai, L. Mezi, D. S. Murra, and C. Zheng, Appl. Phys. B: Lasers Opt. **76**, 277 (2003).
[12] M. Richardson, C.-S. Koay, K. Takenoshita, and C. Keyser, J. Vac. Sci. Technol. B **22**, (2), 758 (2004).
[13] S. Fujioka, H. Nishimura, K. Nishihara, A. Sasaki, A. Sunahara, T. Okuno, N. Ueda, T. Ando, Y. Tao, Y. Shimada, K. Hashimoto, M. Yamaura, K. Shigemori, M. Nakai, K. Nagai, T. Norimatsu, T. Nishikawa, N. Miyanaga, Y. Izawa, and K. Mima, Phys. Rev. Lett. **95**, 235004 (2005).
[14] S. Fujioka, H. Nishimura, K. Nishihara, M. Murakami, Y.-G. Kang, Y. Shimada, A. Sunahara, H. Furukawa, Q. Gu, K. Nagai, T. Norimatsu, N. Miyanaga, Y. Izawa, and K. Mima, Appl. Phys. Lett. **87**, 241503 (2005).
[15] Total masses of the 40 and 1000 nm layer targets are 6.0 and 11.7 μg, respectively. In order to investigate the influence of the target mass on emission distribution, a solid spherical target with a 40 nm Sn overcoat (74.4 μg) was irradiated with the laser pulse, and the spatial distribution similar to that of the hollow substrate sphere was confirmed.